SHALLOW LUNAR SEISMIC ACTIVITY AND THE CURRENT STRESS STATE OF THE MOON

Thomas R. Watters[1], Renee C. Weber[2], Geoffrey C. Collins[3], and Catherine L. Johnson[4,5]

[1]Center for Earth and Planetary Studies, National Air and Space Museum, Smithsonian Institution, Washington, DC 20560, USA
[2]NASA Marshall Space Flight Center, Huntsville, AL 35805, USA
[3]Physics and Astronomy Department, Wheaton College, Norton, MA 02766, USA
[4]Dept. of Earth, Ocean and Atmospheric Sciences, University of British Columbia, Vancouver, British Columbia, V6T 1Z4, Canada
[5]Planetary Science Institute, Tucson, AZ 85719, USA

Introduction

A vast, global network of more than 3200 lobate thrust fault scarps has been revealed in high resolution Lunar Reconnaissance Orbiter Camera (LROC) images (Fig. 1, 2) [1-6]. The fault scarps are very young, <50 Ma, based on their small scale and crisp appearance, crosscutting relations with small-diameter impact craters, and rates of infilling of associated small, shallow graben and may be actively forming today (Fig. 1) [1-3].

The population of young thrust fault scarps provides a window into the recent stress state of the Moon and offers insight into the origin of global lunar stresses. The distribution of orienations of the fault scarps is non-random, inconsistent with isotropic stresses from late-stage global contraction as the sole source of stress. Modeling shows that tidal stresses contribute significantly to the current stress state of the lunar crust [1]. Tidal stresses (orbital recession and diurnal tides) superimposed on stresses from global contraction result in non-isotropic compressional stress and may produce thrust faults consistent with lobate scarp orientations. At any particular point on the lunar surface, peak compressive stress will be reached at a certain time in the diurnal cycle. Coseismic slip events on currently active thrust faults are expected to be triggered when peak stresses are reached. Analysis of the timing of the 28 the shallow moonquakes recorded by the Apollo seismic network (Fig. 2) shows that 19 indeed occur when the Moon is closer to apogee, while only 9 shallow events occur when the Moon is closer to perigee [7]. Here we report efforts to refine the model for the current stress state of the Moon by investigating the contribution of polar wander. Progress on relocating the epicentral locations of the shallow moonquakes using an algorithm designed for sparse networks [12] is also reported.

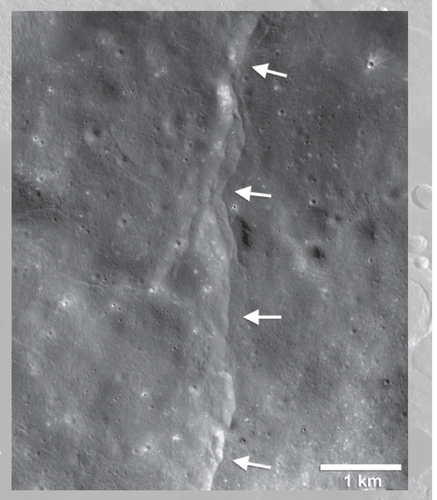

Figure 1. A prominent lobate thrust fault fault scarp in the Vitello Cluster is one of thousands discovered in Lunar Reconnaissance Orbiter Camera images (LROC).

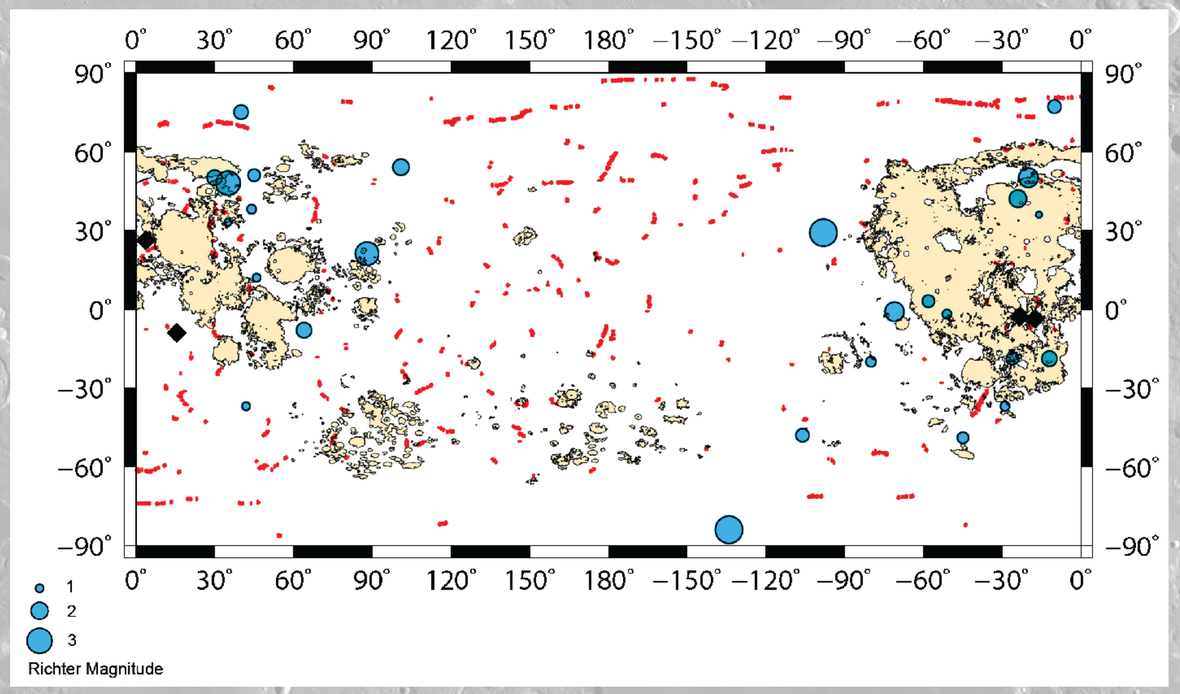

Figure 2. Map of lobate scarps (red), epicentral locations of shallow moonquakes (blue dots) [9], and locations of Apollo Seismic Network seismometers (black diamonds). Moonquakes are scaled by estimated Richter magnitude [10]. Mare basalt units are shown in tan.

Shallow Moonquakes

Four seismometers were placed on the Moon at the Apollo 12, 14, 15 and 16 landing sites. During the operation of the seismometers (1969 to 1977), 28 shallow moonquakes were recorded [9, 10] (Fig. 1). Shallow moonquakes occur at depths <200 km and have been interpreted as tectonic in origin [10]. Analysis of all 28 shallow moonquakes indicates Richter-equivalent magnitudes in the range from 1.6 to 4.2 [10]. Estimates of stress drops range from a few MPa to over 100 MPa for the 3 largest events [11].

The current best estimates for most shallow moonquake locations are likely only accurate to several degrees, possibly more for small and/or distant events. This makes a comparison with stress models and attempts to match the exact locations of known tectonic features with specific shallow moonquakes problematic. Their depths are similarly poorly constrained, with some estimated to occur at the surface, and others up to 200 km deep with uncertainty up to an additional 200 km.

The standard method for locating a seismic event uses a known velocity model and the observed arrival times of the direct P and S waves. Large uncertainties in arrival times directly translate into a large uncertainty in event location. We have instead applied a location algorithm specifically designed for sparse networks [12] to determine whether their location accuracy can be improved. Rather than solving for a best-fit location, this approach divides the solution set into falsified and non-falsified candidate locations using an adaptive grid search, and accounts for arrival time uncertainty using windows around the true arrival time.

Current Stress State and Polar Wander

Radial contraction from interior cooling is the dominant source of stress, contributing ≥2 but <10 MPa based on the currently mapped population of lobate scarps [1, 2]. Superimposed on compressional stresses from contraction σ_c are two components of tidal stress, orbital recession stress σ_r and diurnal stress σ_t. Tidal stresses are dominated by σ_t that may reach 20 to 40 kPa [1]. Stresses due to orbital recession do not change with orbital position, thus it is with the addition of diurnal stresses that peak stresses are reached. At apogee, diurnal and recession stresses are most compressive near the tidal axis, while at perigee they are most compressive 90° away from the tidal axis. Thus, the occurrence of shallow seismic events generated by coseismic slip on the thrust faults may be greater when the Moon is near apogee or perigee [1].

An additional component of stress that may significantly contribute to the current lunar stress state is polar wander. True polar wander has been attributed to a change in the Moon's moments of inertia due to a low-density thermal anomaly beneath Procellarum [8]. The change in the location of the poles is consistent with the observed remnant polar hydrogen deposits [8]. Modeling shows that stresses from ~3° of polar wander σ_w over the last 1 billion years results in stresses with magnitudes up to ±8 kPa (Fig. 3). The net non-isotropic compressional stresses σn from $\sigma_r+\sigma_w+\sigma_c$ result in thrust faults with preferred orientations that are in general agreement with orientations of the mapped faults (Fig. 4). Although the contribution of diurnal tidal stresses to σ_n is small (≤5 kPa), the addition of σ_t results in peak stress when the Moon is near apogee or perigee, consistent with the occurrence of most shallow seismic events [7].

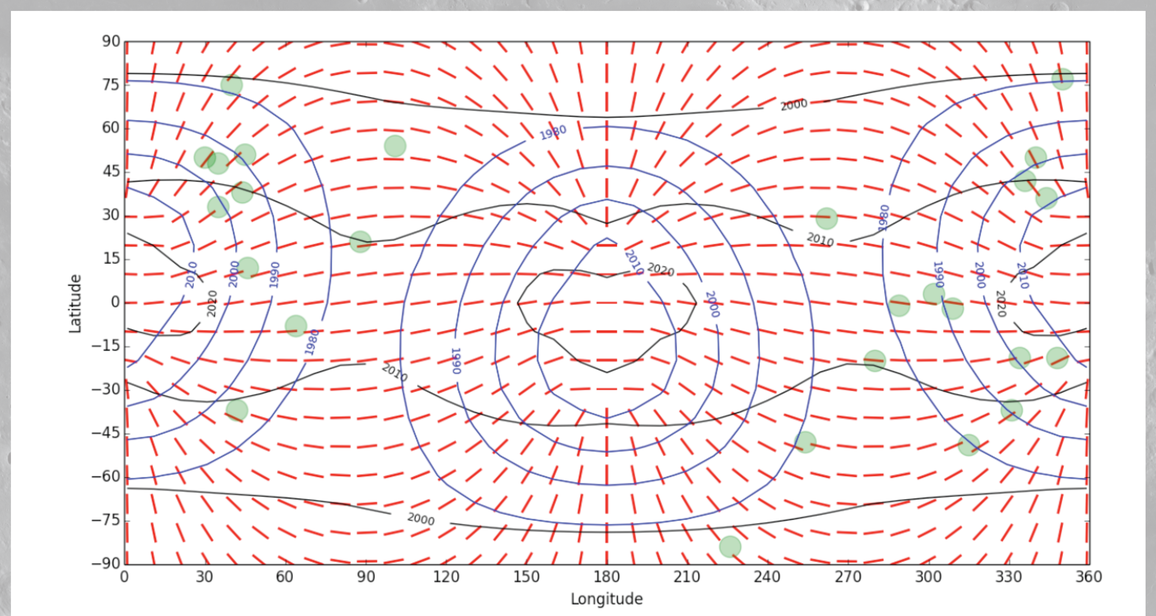

Figure 3. Orientations of principal stresses (red lines) due to 1 B.yr. of orbital recession, 3° of true polar wander, and 2 MPa of isotropic compression from volume contraction (no diurnal tide shown in this plot). Contours of most and least compressive stress magnitudes shown by black and blue lines, respectively. Recession and TPW stresses deviate less than ±25 kPa from the imposed isotropic stress. Moonquake epicenters [9] shown as green circles. Thrust faults would be expected to form perpendicular to the red lines.

Figure 4. Agreement between observed faults and expected local thrust fault orientations due to different stress models. Fault segments at 0° on plot are orthogonal to local direction of most compressive stress, and at 90° they are parallel to most compressive stress.

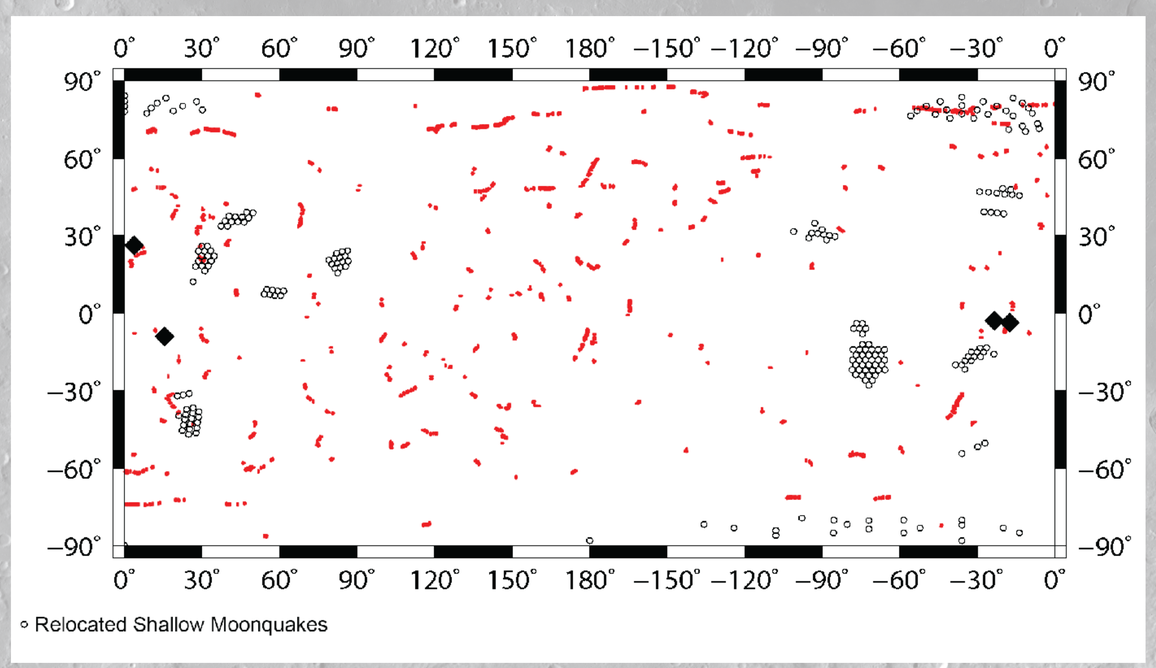

Figure 5. Location clouds of shallow moonquakes with solutions at the surface. Location clouds are indicated by circles (black) and are plotted with the locations of mapped lobate scarps (red). The locations of Apollo Seismic Network seismometers are indicated by diamonds (black).

References

[1] Watters T.R. et al. (2015) Geology, 43, 851–854. [2] Watters T.R. et al. (2010) Science, 329, 936-940. [3] Watters, T.R. et al. (2012) Nature Geoscience, doi:10.1038/NGEO1387. [4] Watters T.R. and Johnson C.L. (2010) in Planetary Tectonics, Cambridge Univ. Press, pp. 121-182. [5] Banks, M. E. et al. (2012) J. Geophys. Res., 117, doi:10.1029/2011JE003907. [6] Williams, N.R. et al. (2013) J. Ge-ophys. Res., doi: 10.1002/jgre.20051. [7] Watters, T.R. et al. (2016) LPSC 47, #1642. [8] Siegler, M.A. et al. (2016) Nature 531, 480-484. [9] Nakamura, Y. et al. (1981) Tech. Rep. 118, Inst. for Geophys., Univ. of Tex. Austin. [10] Nakamura, Y. et al. (1979) Proc. Lunar Sci. Conf. 10, 2299-2309. [11] Oberst, J. (1987) J. Geophys. Res., 92, 1397-1405. [12] Knapmeyer, M. (2008) Geophys. J. Int. 175, 975-991.

Moonquake Relocation

Using the LOCSMITH relocation algorithm [12] adapted for using inaccurate data from very sparse seismic networks, the result for each event is not a single location, but a cloud of candidate locations that are non-falsified (regions where theoretical arrival times fall within arrival time windows for all stations) by any arrival time or back azimuth data (Fig. 5). Of the 28 total shallow moonquakes, 13 have confirmed locations - the location cloud contains the nominal epicentral location, 7 candidates for relocations - the location either moved, or a second location is acceptable (binary cloud), and 8 events are not well constrained - location cloud is fragmented. Acceptable locations occur at depths up to 300 km, beyond which the search was terminated. However, most clouds also include acceptable surface locations. Of the 20 relocated moonquakes with confirmed or binary clouds, 15 have solutions at the surface (Fig. 5).

Visual comparison of the location clouds with mapped lobate scarps indicates at least 6 scarps or scarp clusters are within close spatial proximity to moonquake locations (Fig. 5). These are prime candidates in the search for evidence of recent activity on the young fault scarps. A statistical analysis shows that . . .